Research Article | Vol. 9, No. 4 | 1 Apr 2018 | BIOMEDICAL OPTICS EXPRESS 1735
Biomedical Optics EXPRESS

Hydrogen peroxide and glucose concentration measurement using optical fiber grating sensors with corrodible plasmonic nanocoatings

XUEJUN ZHANG,[1] ZE WU,[2] FU LIU,[3] QIANGQIANG FU,[2] XIAOYONG CHEN,[1] JIAN XU,[1] ZHAOCHUAN ZHANG,[1] YUNYUN HUANG,[1] YONG TANG,[2] TUAN GUO,[1,*] AND JACQUES ALBERT[3]

[1]*Guangdong Provincial Key Laboratory of Optical Fiber Sensing and Communications, Institute of Photonics Technology, Jinan University, Guangzhou 510632, China*
[2]*Guangdong Province Key Laboratory of Molecular Immunology and Antibody Engineering, Department of Bioengineering, Jinan University, Guangzhou 510632, China*
[3]*Department of Electronics, Carleton University, 1125 Colonel by Drive, Ottawa K1S 5B6, Canada*
**tuanguo@jnu.edu.cn*

Abstract: We propose and demonstrate hydrogen peroxide (H_2O_2) and glucose concentration measurements using a plasmonic optical fiber sensor. The sensor utilizes a tilted fiber Bragg grating (TFBG) written in standard single mode communication fiber. The fiber is over coated with an nm-scale film of silver that supports surface plasmon resonances (SPRs). Such a tilted grating SPR structure provides a high density of narrow spectral resonances (Q-factor about 10^5) that overlap with the broader absorption band of the surface plasmon waves in the silver film, thereby providing an accurate tool to measure small shifts of the plasmon resonance frequencies. The H_2O_2 to be detected acts as an oxidant to etch the silver film, which has the effect of gradually decreasing the SPR attenuation. The etching rate of the silver film shows a clear relationship with the H_2O_2 concentration so that monitoring the progressively increasing attenuation of a selected surface plasmon resonance over a few minutes enables us to measure the H_2O_2 concentration with a limit of detection of 0.2 μM. Furthermore, the proposed method can be applied to the determination of glucose in human serum for a concentration range from 0 to 12 mM (within the physiological range of 3-8 mM) by monitoring the H_2O_2 produced by an enzymatic oxidation process. The sensor does not require accurate temperature control because of the inherent temperature insensitivity of TFBG devices referenced to the core mode resonance. A gold mirror coated on the fiber allows the sensor to work in reflection, which will facilitate the integration of the sensor with a hypodermic needle for *in vitro* measurements. The present study shows that Ag-coated TFBG-SPR can be applied as a promising type of sensing probe for optical detection of H_2O_2 and glucose detection in human serum.

OCIS codes: (060.2370) Fiber optics sensors; (240.6680) Surface plasmons; (060.3735) Fiber Bragg gratings.

References and links

1. W. Chen, S. Cai, Q. Q. Ren, W. Wen, and Y. D. Zhao, "Recent advances in electrochemical sensing for hydrogen peroxide: a review," Analyst (Lond.) **137**(1), 49–58 (2012).
2. C. Amatore, S. Arbault, D. Bruce, P. de Oliveira, L. M. Erard, and M. Vuillaume, "Characterization of the electrochemical oxidation of peroxynitrite: relevance to oxidative stress bursts measured at the single cell level," Chemistry **7**(19), 4171–4179 (2001).
3. E. W. Miller, A. E. Albers, A. Pralle, E. Y. Isacoff, and C. J. Chang, "Boronate-based fluorescent probes for imaging cellular hydrogen peroxide," J. Am. Chem. Soc. **127**(47), 16652–16659 (2005).
4. R. Raman and A. Shukla, "A direct borohydride/hydrogen peroxide fuel cell with reduced alkali crossover," Fuel Cells (Weinh.) **7**(3), 225–231 (2007).
5. S. R. Sarathy and M. Mohseni, "The impact of UV/H_2O_2 advanced oxidation on molecular size distribution of chromophoric natural organic matter," Environ. Sci. Technol. **41**(24), 8315–8320 (2007).

#320127 https://doi.org/10.1364/BOE.9.001735
Journal © 2018 Received 19 Jan 2018; revised 1 Mar 2018; accepted 8 Mar 2018; published 15 Mar 2018

Biomedical Optics EXPRESS

6. O. S. Wolfbeis, M. Schäferling, and A. Dürkop, "Reversible optical sensor membrane for hydrogen peroxide using an immobilized fluorescent probe, and its application to a glucose biosensor," Mikrochim. Acta **143**(4), 221–227 (2003).
7. S. Hanaoka, J. M. Lin, and M. Yamada, "Chemiluminescent flow sensor for H_2O_2 based on the decomposition of H_2O_2 catalyzed by cobalt (II)-ethanolamine complex immobilized on resin," Anal. Chim. Acta **426**(1), 57–64 (2001).
8. B. Li, Z. Zhang, and L. Zhao, "Chemiluminescent flow-through sensor for hydrogen peroxide based on sol–gel immobilized hemoglobin as catalyst," Anal. Chim. Acta **445**(2), 161–167 (2001).
9. E. Hurdis and H. Romeyn, Jr., "Accuracy of determination of hydrogen peroxide by cerate oxidimetry," Anal. Chem. **26**(2), 320–325 (1954).
10. C. Matsubara, N. Kawamoto, and K. Takamura, "Oxo [5, 10, 15, 20-tetra (4-pyridyl) porphyrinato] titanium (IV): an ultra-high sensitivity spectrophotometric reagent for hydrogen peroxide," Analyst (Lond.) **117**(11), 1781–1784 (1992).
11. Y. Song, L. Wang, C. Ren, G. Zhu, and Z. Li, "A novel hydrogen peroxide sensor based on horseradish peroxidase immobilized in DNA films on a gold electrode," Sens. Actuators B Chem. **114**(2), 1001–1006 (2006).
12. T. Endo, Y. Yanagida, and T. Hatsuzawa, "Quantitative determination of hydrogen peroxide using polymer coated Ag nanoparticles," Measurement **41**(9), 1045–1053 (2008).
13. E. Filippo, A. Serra, and D. Manno, "Poly (vinyl alcohol) capped silver nanoparticles as localized surface Plasmon resonance-based hydrogen peroxide sensor," Sens. Actuators B Chem. **138**(2), 625–630 (2009).
14. G. L. Wang, X. Y. Zhu, H. J. Jiao, Y. M. Dong, and Z. J. Li, "Ultrasensitive and dual functional colorimetric sensors for mercury (II) ions and hydrogen peroxide based on catalytic reduction property of silver nanoparticles," Biosens. Bioelectron. **31**(1), 337–342 (2012).
15. H. Li, X. Ma, J. Dong, and W. Qian, "Development of methodology based on the formation process of gold nanoshells for detecting hydrogen peroxide scavenging activity," Anal. Chem. **81**(21), 8916–8922 (2009).
16. X. Gao, L. Y. Jin, Q. Wu, Z. C. Chen, and X. F. Lin, "A nonenzymatic hydrogen peroxide sensor based on silver nanowires and chitosan film," Electroanalysis **24**(8), 1771–1777 (2012).
17. B. Yu, J. C. Feng, S. Liu, and T. Zhang, "Preparation of reduced graphene oxide decorated with high density Ag nanorods for non-enzymatic hydrogen peroxide detection," RSC Advances **3**(34), 14303–14307 (2013).
18. S. Chen, R. Yuan, Y. Chai, and F. Hu, "Electrochemical sensing of hydrogen peroxide using metal nanoparticles: a review," Mikrochim. Acta **180**(1–2), 15–32 (2013).
19. J. Ju and W. Chen, "In situ growth of surfactant-free gold nanoparticles on nitrogen-doped graphene quantum dots for electrochemical detection of hydrogen peroxide in biological environments," Anal. Chem. **87**(3), 1903–1910 (2015).
20. Y. Li, J. B. Zheng, Q. L. Sheng, and B. N. Wang, "Synthesis of Ag@AgCl nanoboxes, and their application to electrochemical sensing of hydrogen peroxide at very low potential," Mikrochim. Acta **182**(1–2), 61–68 (2015).
21. H. Razmi, R. Mohammad-Rezaei, and H. Heidari, "Self-assembled prussian blue nanoparticles based electrochemical sensor for high sensitive determination of H_2O_2 in acidic media," Electroanalysis **21**(21), 2355–2362 (2009).
22. C. K. Tagad, H. U. Kim, R. Aiyer, P. More, T. Kim, S. H. Moh, A. Kulkarni, and S. G. Sabharwal, "A sensitive hydrogen peroxide optical sensor based on polysaccharide stabilized silver nanoparticles," RSC Advances **3**(45), 22940–22943 (2013).
23. C. Zhang, L. Li, J. Ju, and W. Chen, "Electrochemical sensor based on graphene-supported tin oxide nanoclusters for nonenzymatic detection of hydrogen peroxide," Electrochim. Acta **210**, 181–189 (2016).
24. C. Caucheteur, T. Guo, and J. Albert, "Review of plasmonic fiber optic biochemical sensors: improving the limit of detection," Anal. Bioanal. Chem. **407**(14), 3883–3897 (2015).
25. C. K. Tagad, S. R. Dugasani, R. Aiyer, S. Park, A. Kulkarni, and S. Sabharwal, "Green synthesis of silver nanoparticles and their application for the development of optical fiber based hydrogen peroxide sensor," Sens. Actuators B Chem. **183**(5), 144–149 (2013).
26. P. Bhatia, P. Yadav, and B. D. Gupta, "Surface plasmon resonance based fiber optic hydrogen peroxide sensor using polymer embedded nanoparticles," Sens. Actuators B Chem. **182**, 330–335 (2013).
27. J. Albert, L. Y. Shao, and C. Caucheteur, "Tilted fiber Bragg grating sensors," Laser Photonics Rev. **7**(1), 83–108 (2013).
28. T. Erdogan and J. E. Sipe, "Tilted fiber phase gratings," J. Opt. Soc. Am. A **13**(2), 296–313 (1996).
29. G. Laffont and P. Ferdinand, "Tilted short-period fiber-Bragg grating induced coupling to cladding modes for accurate refractometry," Meas. Sci. Technol. **12**(7), 765–770 (2001).
30. C. Caucheteur, C. Chen, V. Voisin, P. Berini, and J. Albert, "A thin metal sheath lifts the EH to HE degenercacy in the cladding mode refractometric sensitivity of optical fiber sensors," Appl. Phys. Lett. **99**(4), 041118 (2011).
31. T. Guo, F. Liu, Y. Liu, N. K. Chen, B. O. Guan, and J. Albert, "In-situ detection of density alteration in non-physiological cells with polarimetric tilted fiber grating sensors," Biosens. Bioelectron. **55**, 452–458 (2014).
32. T. Guo, F. Liu, X. Liang, X. Qiu, Y. Huang, C. Xie, P. Xu, W. Mao, B. O. Guan, and J. Albert, "Highly sensitive detection of urinary protein variations using tilted fiber grating sensors with plasmonic nanocoatings," Biosens. Bioelectron. **78**, 221–228 (2016).
33. Y. Y. Shevchenko and J. Albert, "Plasmon resonances in gold-coated tilted fiber Bragg gratings," Opt. Lett. **32**(3), 211–213 (2007).

Biomedical Optics EXPRESS

34. Y. Yuan, T. Guo, X. Qiu, J. Tang, Y. Huang, L. Zhuang, S. Zhou, Z. Li, B. O. Guan, X. Zhang, and J. Albert, "Electrochemical surface plasmon resonance fiber-optic sensor: in situ detection of electroactive biofilms," Anal. Chem. **88**(15), 7609–7616 (2016).
35. V. Malachovská, C. Ribaut, V. Voisin, M. Surin, P. Leclère, R. Wattiez, and C. Caucheteur, "Fiber-optic SPR immunosensors tailored to target epithelial cells through membrane receptors," Anal. Chem. **87**(12), 5957–5965 (2015).
36. Y. Shevchenko, T. J. Francis, D. A. D. Blair, R. Walsh, M. C. DeRosa, and J. Albert, "In Situ biosensing with a surface plasmon resonance fiber grating aptasensor," Anal. Chem. **83**(18), 7027–7034 (2011).
37. L. A. Obando and K. S. Booksh, "Tuning dynamic range and sensitivity of white-Light, multimode, fiber-optic surface plasmon resonance sensors," Anal. Chem. **71**(22), 5116–5122 (1999).
38. C. Caucheteur, V. Voisin, and J. Albert, "Near-infrared grating-assisted SPR optical fiber sensors: design rules for ultimate refractometric sensitivity," Opt. Express **23**(3), 2918–2932 (2015).
39. H. Neff, W. Zong, A. Lima, M. Borre, and G. Holzhüter, "Optical properties and instrumental performance of thin gold films near the surface plasmon resonance," Thin Solid Films **496**(2), 688–697 (2006).
40. X. L. Yu, D. X. Wang, and Z. B. Yan, "Simulation and analysis of surface plasmon resonance biosensor based on phase detection," Sens. Actuators B Chem. **91**(1), 285–290 (2003).
41. J. Lu, R. F. Bu, Z. L. Sun, Q. S. Lu, H. Jin, Y. Wang, S. H. Wang, L. Li, Z. L. Xie, and B. Q. Yang, "Comparable efficacy of self-monitoring of quantitative urine glucose with self-monitoring of blood glucose on glycaemic control in non-insulin-treated type 2 diabetes," Diabetes Res. Clin. Pract. **93**(2), 179–186 (2011).
42. M. S. Steiner, A. Duerkop, and O. S. Wolfbeis, "Optical methods for sensing glucose," Chem. Soc. Rev. **40**(9), 4805–4839 (2011).
43. A. Deep, U. Tiwari, P. Kumar, V. Mishra, S. C. Jain, N. Singh, P. Kapur, and L. M. Bharadwaj, "Immobilization of enzyme on long period grating fibers for sensitive glucose detection," Biosens. Bioelectron. **33**(1), 190–195 (2012).
44. B. Luo, Z. Yan, Z. Sun, J. Li, and L. Zhang, "Novel glucose sensor based on enzyme-immobilized 81° tilted fiber grating," Opt. Express **22**(25), 30571–30578 (2014).
45. B. Q. Jiang, K. M. Zhou, C. L. Wang, Q. Z. Sun, G. L. Yin, Z. J. Tai, K. Wilson, J. L. Zhao, and L. Zhang, "Label-free glucose biosensor based on enzymatic graphene oxide-functionalized tilted fiber grating," Sens. Actuators B Chem. **254**, 1033–1039 (2018).
46. C. Yeh and G. Lindgren, "Computing the propagation characteristics of radially stratified fibers: an efficient method," Appl. Opt. **16**(2), 483–493 (1977).
47. P. B. Johnson and R. W. Christy, "Optical Constants of the Noble Metals," Phys. Rev. B **6**(12), 4370–4379 (1972).

1. Introduction

The detection of hydrogen peroxide, H_2O_2, at low concentration is an important analytical task due to its importance in pharmaceutical, clinical, environment, mining, textile and food manufacturing applications. For example, H_2O_2 is a toxic by-product of many biological oxidases [1] in which H_2O_2 has been considered to be an indicator of diseases such as Parkinson's disease, cancer, stroke, arteriosclerosis and Alzheimer's disease [2, 3]. In addition, H_2O_2 has been used in liquid-based fuel cells and in organic synthesis because it is a powerful oxidizing agent [4, 5]. Therefore, it is important for both academic research and industrial purposes to be able to detect and accurately measure H_2O_2 concentration. To date, various analytical techniques have been developed for this task, such as fluorescence [6] chemiluminescence [7, 8], titration [9], spectrophotometry [10], and electrochemical techniques [11], Some surface plasmon resonance (SPR) devices based on different surface functionalized nanomaterials such as nanoparticles [12–14] nanoshells [15] nanowires [16] and nanorods [17] have been used to quantitatively determine H_2O_2 concentration. In the case of SPR, the absorption strength decreases because of the metal oxidation by the H_2O_2. Most of above methods provide benefits of simplicity, speed, high sensitivity and reliability, and therefore are widely used for *in vitro* detection with a limit of detection (LOD) of about a micromole per liter (μM) in the laboratory [18–23]. However, the sample preparation for existing measurement techniques is relatively time-consuming and the measurements are vulnerable to environmental influences such as temperature, dust, spatial light coupling fluctuations.

The optical fiber sensors have significant advantages, such as small size, cost-effectiveness, multiplexing ability and remote operation ability, and have been widely studied in pharmaceuticals, healthcare, biomedical research, and environmental protection. Therefore, SPR based fiber optic sensors have gained considerable attention in bio-chemical fields due to

Biomedical Optics EXPRESS

their unique characteristics such as fast response, high sensitivity and label-free detection [24]. For example, H_2O_2 measurement based on etching of metal on a polymer fiber stripped of its cladding and bent into a U-shape [25] and polyvinyl alcohol (PVA) embedded silver nanoparticles over the silver coated core of the optical fiber [26] have been reported. However, such configurations considerably weaken the mechanical strength of the fiber and require careful individual fabrication, thereby limiting their use in practical applications. To overcome this problem, a new kind of fiber grating sensor, the tilted fiber Bragg grating (TFBG), has been developed and studied [27] based on original work in other fields [28, 29]. These are short period (~500 nm) gratings with light-induced refractive index modulation planes slightly inclined with respect to the cross-section of the optical fiber. There is no structural damage to the fiber, so the reproducibility and sensing stability can be guaranteed. The tilted grating also breaks the cylindrical symmetry of standard fibers, resulting in a strong polarization selectivity of the TFBG's excited cladding modes. When the fiber cladding over the TFBG is coated with a thin metal layer, radially polarized cladding modes can excite surface plasmon resonances (SPRs) at the interface between the metal and the surrounding dielectric.

Such TFBG-SPR structures enable measurements of changes in the refractive index (RI) in proximity to the surface of the fiber with resolution down to 10^{-5} refractive index units (RIUs) [30–33]. Finally, the most important feature of TFBG-SPR devices for sensing is the presence in the transmission spectrum of a resonance that is insensitive to the surrounding RI but sensitive to the temperature (with a very well calibrated sensitivity of ~10 pm/°C). This resonance can be used as an in situ thermometer to calibrate out this effect on the results, and as a power level reference in the same measurement that is used to sense the surface refractive index.

Most of the reported SPR based optical fiber sensors so far are based on a metal film with fixed thickness [34–37]. However, the thickness of the metal film itself can be used as a changeable parameter for high resolution measurement, especially for surrounding refractive index (SRI) measurement [38–40] Instead of the traditional measurement technique, where the wavelength shift of the SPR attenuation is monitored, here we propose a much simpler sensing method of monitoring the rate of change of the attenuation induced by the SPR. We will show that the rate of change is directly related to the H_2O_2 concentration. The operating principle is that H_2O_2 will etch the silver coating of the TFBG, reducing its thickness, so that the SPR-induced attenuation of the fiber cladding resonances decreases and eventually disappears. In this way, the attenuation of the narrow cladding modes whose wavelengths are matched to the SPR attenuation band can be used to monitor the concentration of the H_2O_2.

Besides monitoring H_2O_2, we further propose a simple and *in vitro* method to measure glucose in human serum by the same approach. The continuous interest in sensing glucose, mainly in blood, is due to the increase of incidence of diabetes resulting from aging and unhealthy diets. Diabetic mellitus, which results from insulin deficiency and hyperglycemia can be detected when blood glucose concentrations deviate from the normal range of 80-120 mg/dL (4.4-6.6 mM) [41]. The proposed detection scheme is based on the effect of enzymatic oxidation, whereby the glucose in human serum will react with added glucose oxidase (Gox) to produce H_2O_2. Since the etching rate of the silver coating is proportional to the concentration of the glucose, this can be detected by spectral monitoring of the SPR attenuation in reflection. Compared with the traditional electrochemical method for sensing glucose, our method is capable of remote operation ability and multiplexing [42]. Moreover, in comparison with the other optical fiber methods, the response time of our proposed method is only 20 minutes and no enzyme treatment is required on the surface of the fiber [43–45].

Biomedical Optics EXPRESS

2. Materials and method

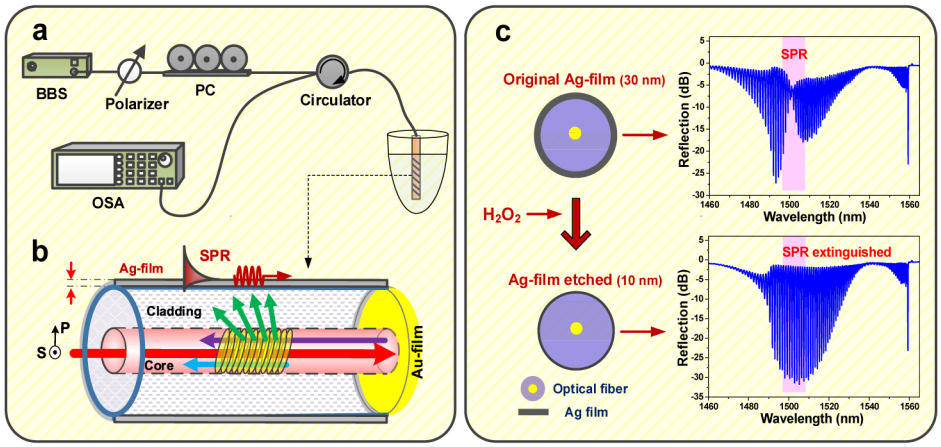

Fig. 1. Ag-coated TFBG-SPR system: (a) experimental setup of glucose detection; (b) schematic diagram of the Ag-coated TFBG-SPR biosensor interrogated with tunable linearly polarized light; (c) the reflection spectrum before and after etching.

2.1 Materials and equipment preparation

Serum samples were collected from the Cancer Center of the First Affiliated Hospital of Jinan University (Guangzhou, China). The phosphate buffer solution (PBS, PH 7.4), Hydrogen peroxide (H_2O_2, 30 wt. %) and glucose sample were bought from GZ Chemical Reagent (Guangzhou, China), and the glucose oxidase (GOx) was purchased from Sigma-Aldrich. Ultrapure water (Milli-Q grade, Millipore) with a resistivity of 18.2 MΩ/cm was used throughout this study. A scanning electron microscope and a centrifuge (Beckman, Germany) were used, as well as an Atomic force microscope (AFM, Bruker, USA). Silver coatings on fibers were produced with a magnetron sputtering coating machine (SKY TEACHNOLOGY DEVELOPMENT, China).

2.2 Sensor configuration and principle

The experimental setup for H_2O_2 measurement is based on an Ag-coated 18°-tilt TFBG (diameter: 125 μm; length: 2 cm) as presented in Fig. 1(a). Here, the plasmonic TFBG sensor was powered by a broadband source (BBS) with wavelength range of 1460-1560 nm and its reflection spectrum was monitored by an optical spectrum analyzer (OSA) with wavelength resolution of 0.02 nm. A linear polarizer and a polarization controller (PC) were placed upstream of the circulator to adjust the orientation of input light polarization (P-polarization relative to the tilted planes of the grating, in Fig. 1(b)), so as to provide the strongest SPR excitation, i.e. selective excitation of cladding modes with almost 100% radially polarized light at the cladding surface. The measured results were recorded continuously every 1.2 seconds. Figure 1(b) shows the configuration of the Ag-coated TFBG probe. The tilt of the grating is an important parameter since it can be used to choose which set of cladding modes is to be excited [27]. As a result, it is possible to adjust the operating range of the sensor in order to optimize the response for certain refractive indices. In this work, the tilt angle of TFBG was selected to be 18°, which provides the maximum amplitude for cladding modes in aqueous solution measurements with RI range of 1.32-1.34.

A 32 nanometer thick silver film was deposited on the fiber by radio frequency magnetron sputtering. To ensure adequate adhesion of the silver film, we deposited a 2 to 3 nm film of chromium on the fiber prior to silver deposition. Azimuthal uniformity of the silver film thickness over the fiber surface was achieved by rotating fiber around its axis during the sputtering process. A thin gold mirror was coated on fiber tip surface to enable interrogation

Biomedical Optics EXPRESS

of the sensor in reflection, allowing the sensor to be simply inserted into the solution under test. Finally, the gold mirror is protected with a deposited layer of 500 nm of SiO_2 on the fiber tip by radio frequency (RF) magnetron sputtering. This effectively eliminates external influences and keeps the reflection spectrum much more stable.

Figure 1(c) illustrates the sensing principle of the H_2O_2 sensor. Following immersion of the TFBG coated with 30 nm of silver into the H_2O_2 solution, the thickness of the silver film progressively decreases with the H_2O_2 etching time. The decreasing thickness of the metal film broadens and weakens the SPR resonance of the metal-SRI boundary and causes a progressive recovery of the amplitudes of the SPR attenuated cladding mode resonances. Since the etching rate of silver shows a clear relationship with the prepared H_2O_2 concentration, we can measure this concentration by monitoring the rate of recovery of the cladding mode amplitudes, following a suitable calibration.

3. Theoretical analysis and demonstration

To further study the relationship between the SPR mode and the thickness of silver film coated over the fiber, we numerically calculate the SPR excitation through a finite-difference complex mode solver using the FIMMWAVE software. This software will model fibers of arbitrary (real) RI, using a rigorous solution to the vectorial wave equation in cylindrical co-ordinates. The solution assumes isotropic media and either an infinite cladding layer or with a perfect electrical conductor as the outer boundary condition [46].

A four-layered waveguide was constructed with the following parameters: fiber grating with title angle of 18 degree and grating pitch of 557 nm; fiber core with refractive index of 1.4498 and diameter of 8.2 μm; fiber cladding with refractive index of 1.4440 and diameter of 125 μm; fiber cladding surrounded by a silver sheath with a complex refractive index (n_{silver} = 0.139-i10.963) [47] and thickness over the range from 0 to 30 nm; the silver sheath is surrounded by 80 μm water layer with refractive index of 1.3154 (the nominal RI of water was calculated at the wavelength of 1550 nm, not 589 nm Abbe refractometer).

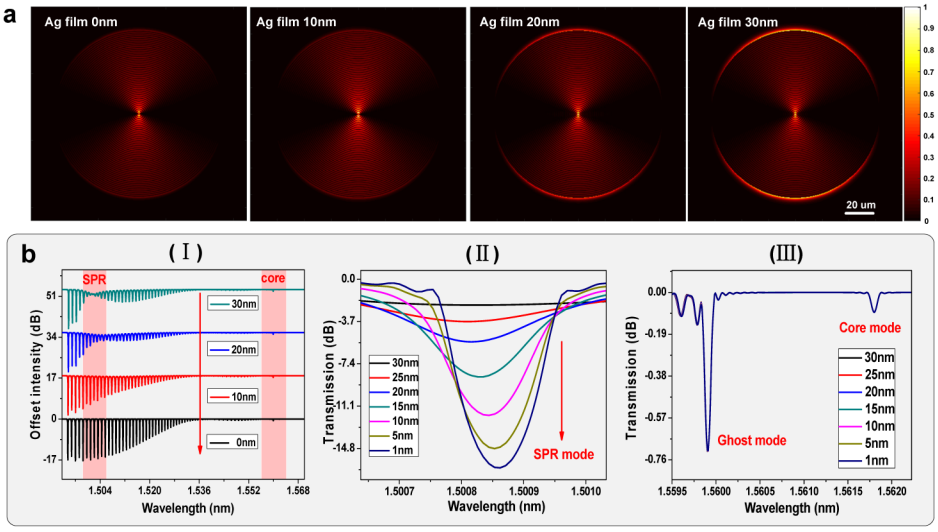

Fig. 2. a) Simulated mode intensity profiles of a cladding mode phase matched to the silver-water interface SPR; b) Simulated transmission spectra of 18° tilted FBG for different Ag thicknesses according to the legends: I full spectrum; II SPR matched cladding mode; III low order cladding modes and core mode (details in the text).

We numerically simulated radially polarized modes ("EH" in the accepted mode nomenclature) to get the mode intensity profiles shown in Fig. 2(a). As we can see, a cladding mode with strong SPR-induced field localization near the coating boundary can be found

Biomedical Optics EXPRESS

when the silver layer has a thickness of 30 nm. The SPR nature of this mode can be further confirmed by the fact that its propagation constant is found to have the largest imaginary part, corresponding to the maximum loss. Also, evident from the simulation is that the SPR excitation becomes weaker and weaker when the thickness of silver layer decreases. Such strong modulation of SPR efficiency numerically demonstrates the feasibility of our proposed sensor. Further simulations of actual TFBG-SPR transmission spectra (carried out with an in house numerical tool) are shown in part I of Fig. 2(b), for four different thicknesses of silver, EH modes, and water surroundings. The SPR-induced attenuation of the cladding mode resonance becomes weaker and spectrally broadened. Therefore, a selected cladding mode located near the center of the SPR attenuation band becomes stronger and deeper as the silver thickness decreases (Fig. 2bII). As expected however, low order cladding modes (the so-called "ghost" mode) and the core mode resonance remain unchanged (Fig. 2bIII).

4. Results and discussion

4.1 Surface morphology of silver film

Figure 3 gives us the initial thickness of silver on TFBG which is not etched by H_2O_2 solution. The film includes chromium and silver, and the total thickness is about 32 nm. Optimizing thickness of silver coatings on TFBG for H_2O_2 application is demonstrated by the simulation. Figure 4 shows the surface morphologies of a 30-nm thick silver film (obtained by atomic force microscopy) with etching times of 0, 10 and 30 minutes in 2 mM H_2O_2 in water. It is clear that the originally smooth Ag film gradually changes to a coarse surface with different sizes of nanoparticles. The longer the etch time the rougher and the thinner of the silver film is. As the silver film becomes thinner, the SPR attenuation profile (dashed lines) becomes weaker and spectrally broadened as predicted by simulations.

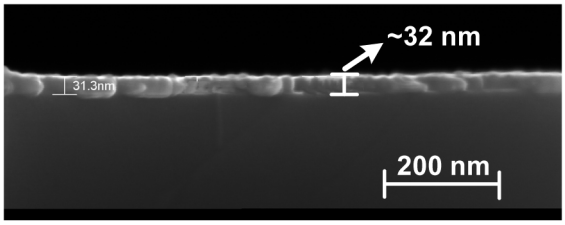

Fig. 3. SEM of the initial thickness of silver on TFBG without etching.

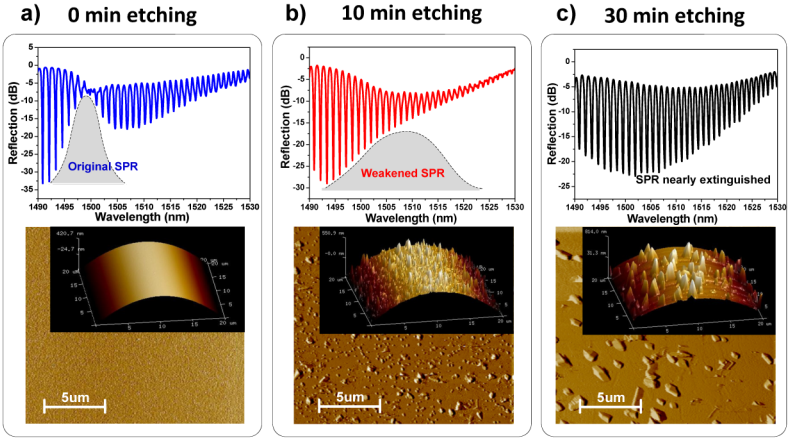

Fig. 4. Experimentally measured spectral response of Ag-coated TFBG and the corresponding surface morphologies of silver film versus different etching times in 2 mM H_2O_2 in water.

Biomedical Optics EXPRESS

4.2 Detection of H_2O_2

Figure 5 presents the spectral response of a 30 nm Ag-coated TFBG sensor when it was immersed in a 2000 μM H_2O_2 solution. Figure 5(a) shows the full reflection spectrum of the sensor. There are two regions of interest: From 1450 to 1550 nm the Ag film etching induced SPR modulation and the corresponding cladding modes changes are evident (gray shadow area), and near 1559 nm, we observe the unchanged "ghost" mode (a group of strongly guided cladding modes which interact with cladding-metal interface but little with the outside medium) and core mode used for self-calibration (blue shadow area). Figure 5(b) presents the zoomed spectral response of the selected cladding mode measured each minute during a 30-minute H_2O_2 etch. The selected cladding mode becomes stronger and deeper as the SPR attenuation decreases due to the silver etching. Whilst the cladding modes in the SPR area change significantly with time due to silver film etching, the ghost and core modes remain unchanged, as shown in Fig. 5(c), because they are insensitive to the SRI. The ghost and core modes can be used to calibrate the effect of temperature and to eliminate power fluctuation from the measurement, thus improving the stability and accuracy of the sensor.

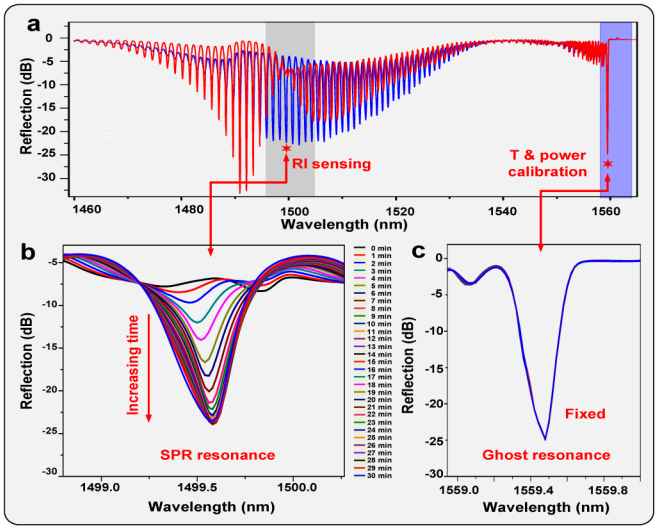

Fig. 5. Experimental spectra during H_2O_2 etching at times indicated in the legend: (a) Response of 30 nm Ag-coated TFBG immersed in a 2000 μM H_2O_2 solution; (b) and (c) are the zoomed spectra of the SPR attenuated cladding mode and the ghost mode, respectively.

The optical fiber sensor response for different concentrations of H_2O_2 is shown in Fig. 6. Figure 6(a) depicts the SPR intensity change versus H_2O_2 concentration during a one hour etch. Note that the selected cladding mode for monitoring is chosen as the most attenuated resonance on the original spectrum. We can see that the reaction speeds up as the concentration increases but that it saturates after a certain time. Therefore, for the detection of lower concentrations of H_2O_2, a much longer response time is required. Furthermore, we can see that when the concentration is as low as 0.2 μM, it becomes difficult to observe an amplitude change on the scale of the figure, which means that the concentration of H_2O_2 is too low to etch the silver film significantly within a limited time (one hour here). To calibrate the sensor response in terms of amplitude recovery rate vs concentration, the resonance amplitude at the arbitrarily determined time of 20 minutes was chosen. The resulting resonance amplitude recovery (normalized to the initial resonance amplitude) as a function of concentration of H_2O_2 is shown in Fig. 6(b). This clearly shows that the SPR attenuation of the resonance amplitude decreases nonlinearly but monotonically with the concentration of H_2O_2 in the range from 0.2 μM to 5000 μM. In particular, it will be shown in Section 4.4 that

Biomedical Optics EXPRESS

for glucose concentrations in the physiological range from 3 to 8 mM, the concentration of H_2O_2 produced by enzymatic oxidation falls between 1 and 20 μM, corresponding to amplitude recoveries between 1 and 5 dB (cross-hatched area in Fig. 6(b)). Of course, the proposed biosensor is designed as a disposable sensor (once the silver film is etched, the sensor no longer works). However, it is re-usable simply by depositing a new coating. In our lab, we use a mixed solution of 50 g of ceric ammonium nitrate (CAN) dissolved in 13 ml perchloric acid (PA) and 200ml deionized water solution to refresh the fiber surface (including removal the residual Cr) prior to re-deposition.

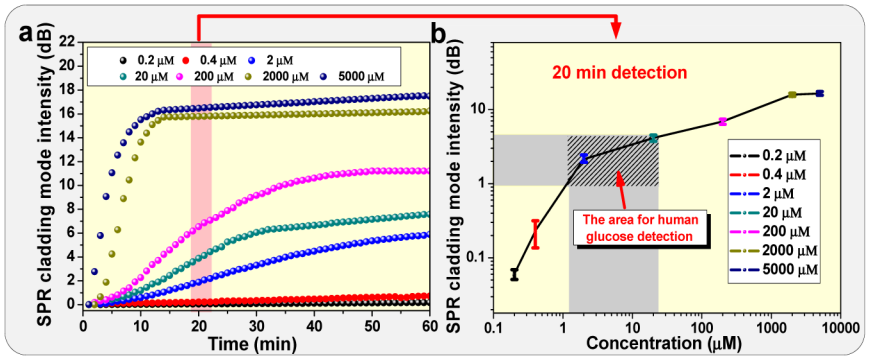

Fig. 6. Responses of the plasmonic TFBG versus H_2O_2 solutions at different concentrations: (a) real time intensity responses of cladding mode near 1500 nm in Fig. 5; (b) Normalized amplitude recovery, in dB relative to the initial amplitude, for different H_2O_2 concentrations after 20 minutes of etch time.

4.3 Glucose detection in human serum

Unlike the traditional plasmonic fiber-optic sensors discussed, here we can also take advantage of the weakening of the surface Plasmon resonance in the presence of H_2O_2 for glucose measurements. When the D-glucose contained in human serum is mixed with a proper oxidant (GOx.), H_2O_2 will be produced by enzymatic oxidation and etch the silver coating as described above.

The enzymatic oxidation between the D-glucose and GOx to generate H_2O_2 can be described by Eqs. (1) and (2):

$$\mathrm{D-glucose} + \mathrm{O_2} + \mathrm{H_2O} \xrightarrow{\mathrm{GOx}} \mathrm{D-glucodic\ acid} + \mathrm{H_2O_2} \quad (1)$$

$$2\mathrm{Ag} + \mathrm{H_2O_2} \rightarrow 2\mathrm{Ag^+} + 2\mathrm{OH^-} \quad (2)$$

Experiments were carried out with glucose at different concentrations from 0 mM to 12 mM in serum solutions (serum in PBS, diluted 10 times). In each case, 500 μL of 10 μM glucose oxidase was transferred into 4.5 mL of the mixed solution. The glucose and GOx concentrations are allowed to reach steady state in solution before the sensor is introduced.

For each glucose mix solution, the silver coated TFBG is immersed and its spectrum monitored for 20 minutes. The change in amplitude of the 1500 nm resonance over this period is plotted in Fig. 7, as a function of the actual glucose concentration measured separately with a commercial glucometer (SANNUO quasi). Three times repeated measurements were used to quantify the measurement performance with a relative standard deviation (RSD) of less than 15%.

These results can be used to calibrate the responsivity of our proposed plasmonic fiber-optic sensor, yielding a glucose concentration sensitivity of 0.5 dB/mM at a detection time of 20 minutes.

Biomedical Optics EXPRESS

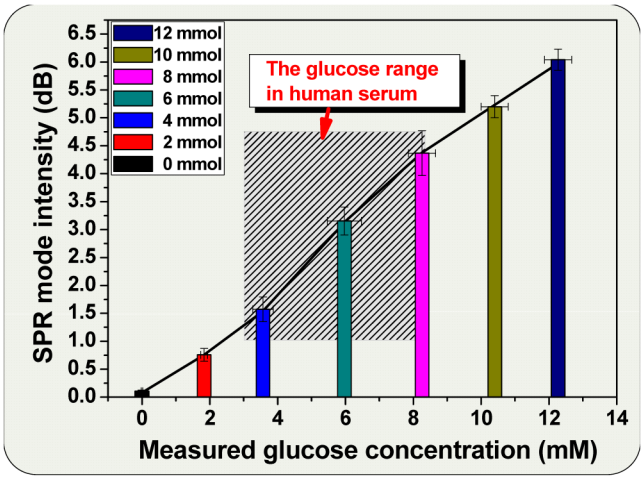

Fig. 7. Amplitude recovery of the SPR resonance near 1500 nm for different glucose concentrations in human serum at 20 minutes response time.

5. Conclusion

We have proposed and experimentally demonstrated an Ag-coated plasmonic TFBG sensor for H_2O_2 concentration measurement. Through monitoring the amplitude change of a selected cladding mode within the wavelength band of the Ag-water SPR, a concentration of H_2O_2 as low as 0.2 μM can be detected, thanks to inherent self-calibration using other, un-sensitive resonances in the measured data. Furthermore, taking advantage of the unique optical properties of the etching effect of H_2O_2 generated from the enzymatic oxidation of glucose, we have successfully demonstrated a new method for *in vitro* measurement of glucose in human serum. The high sensitivity together with the miniaturized size, remote operation and label-free detection may make the proposed sensor a good candidate for biochemical detection involving the generation of H_2O_2.

Funding

National Natural Science Foundation-Excellent Youth Foundation of China (No. 61722505); the Guangdong Youth Science and Technology Innovation Talents of China (No. 2014TQ01X539); Guangzhou Key Collaborative Innovation Foundation of China (No. 2016201604030084); Natural Sciences and Engineering Research Council of Canada (No. RGPIN 2014-05612); Canada Research Chairs Program (No. 950-217783).

Disclosures

The authors declare that there are no conflicts of interest related to this article.